Search Content

Search by Title, Abstract, Keywords or DOI

Search Authors

Search by Surname, Initials or Email

Volume 17 Number 6, June 2018

Original Research Article

Development of fast-release piroxicam/polyethylene glycol capsules by solid dispersion and curing using full factorial design HTML (abstract.php?id=2152&aTitle=Development of fast-release piroxicam/polyethylene glycol capsules by solid dispersion and curing using full factorial design) | Fulltext (../admin/12389900798187/2018_17_6_1.pdf)

Benchawan Chamsai, *Wipada Samprasit* (mailto:swipada@hotmail.com),

http://dx.doi.org/10.4314/tjpr.v17i6.1
(http://dx.doi.org/10.4314/tjpr.v17i6.1)

Hydroxypropyl cellulose-based orally disintegrating films of promethazine HCl for the treatment of motion sickness HTML (abstract.php?id=2153&aTitle=Hydroxypropyl cellulose-based orally disintegrating films of promethazine HCl for the treatment of motion sickness) | Fulltext (../admin/12389900798187/2018_17_6_2.pdf)

Amjad Hussain (mailto:amjad_husein@hotmail.com), *Sadia Latif*, *Nasir Abbas*, *Muhammad Irfan*, *Muhammad Sohail Arshad*, *Nadeem Irfan Bukhari*,

http://dx.doi.org/10.4314/tjpr.v17i6.2
(http://dx.doi.org/10.4314/tjpr.v17i6.2)

Co-crystalization of quercetin and malonic acid using solvent-drop grinding method HTML (abstract.php?id=2154&aTitle=Co-crystalization of quercetin and malonic acid using solvent-drop grinding method) | Fulltext (../admin/12389900798187/2018_17_6_3.pdf)

Dwi Setyawan (mailto:dwisetyawan-90@ff.unair.ac.id), *Rachel Olivia Jovita*, *Muhammad Iqbal*, *Abhimata Paramanandana*, *Helmy Yusuf*, *Maria LAD Lestari*,

http://dx.doi.org/10.4314/tjpr.v17i6.3
(http://dx.doi.org/10.4314/tjpr.v17i6.3)

N-(4-hydroxyphenyl) retinamide inhibits migration of renal carcinoma cells and promotes autophagy via MAPK p38 pathway HTML (abstract.php?id=2155&aTitle=N-(4-

hydroxyphenyl) retinamide inhibits migration of renal carcinoma cells and promotes autophagy via MAPK p38 pathway) | Fulltext (../admin/12389900798187/2018_17_6_4.pdf)

Jianguo Gao, Jianer Tang, Yu Chen, Junwen Shen, Ning Wang, Zhihai Fang, Guiqin Shen, Fan Ren, Rongjiang Wang (mailto:rongjiangwang@hotmail.com),

http://dx.doi.org/10.4314/tjpr.v17i6.4
(http://dx.doi.org/10.4314/tjpr.v17i6.4)

Taraxerol exerts potent anticancer effects via induction of apoptosis and inhibition of Nf-kB signalling pathway in human middle ear epithelial cholesteatoma cells HTML (abstract.php?id=2156&aTitle=Taraxerol exerts potent anticancer effects via induction of apoptosis and inhibition of Nf-kB signalling pathway in human middle ear epithelial cholesteatoma cells) | Fulltext (../admin/12389900798187/2018_17_6_5.pdf)

Jun Liao (mailto:janetsntal@yahoo.com), *Fengfang Wu, Wen Lin, Zhiwei Huang,*

http://dx.doi.org/10.4314/tjpr.v17i6.5
(http://dx.doi.org/10.4314/tjpr.v17i6.5)

Vasodilator effect of 1-trifluoromethoxyphenyl-3-(1-propionylpiperidin-4-yl) urea is predominantly mediated through activation of voltage-dependent K+ channels HTML (abstract.php?id=2157&aTitle=Vasodilator effect of 1-trifluoromethoxyphenyl-3-(1-propionylpiperidin-4-yl) urea is predominantly mediated through activation of voltage-dependent K+ channels) | Fulltext (../admin/12389900798187/2018_17_6_6.pdf)

Shafiq Ali Shah, Malik Hassan Mehmood (mailto:malikhassan.mehmood@gmail.com), *Munasib Khan, Ishfaq Ali Bukhari, Anwarul Hassan Gilani,*

http://dx.doi.org/10.4314/tjpr.v17i6.6
(http://dx.doi.org/10.4314/tjpr.v17i6.6)

Antioxidant and hepatoprotective effects of vitamin E and melatonin against copper-induced toxicity in rats HTML (abstract.php?id=2158&aTitle=Antioxidant and hepatoprotective effects of vitamin E and melatonin against copper-induced toxicity in rats) | Fulltext (../admin/12389900798187/2018_17_6_7.pdf)

Mehmet Ali Temiz (mailto:matemiz@yyu.edu.tr), *Atilla Temur, Elif Kaval Oguz,*

http://dx.doi.org/10.4314/tjpr.v17i6.7
(http://dx.doi.org/10.4314/tjpr.v17i6.7)

Evaluation of biochemical constituents and inhibitory effect of tea clone 100 on colorectal cancer cell line HCT-116 HTML (abstract.php?id=2159&aTitle=Evaluation of biochemical constituents and inhibitory effect of tea clone 100 on colorectal cancer cell line HCT-116) | Fulltext (../admin/12389900798187/2018_17_6_8.pdf)

Fereydoon Bondarian, Asa Ebrahimi (mailto:dr.asaebrahimi@gmail.com), *Frouzandeh Mahjoubi, Eslam Majidi Hervan, Azadi Gonbad,*

http://dx.doi.org/10.4314/tjpr.v17i6.8
(http://dx.doi.org/10.4314/tjpr.v17i6.8)

Antiproliferative and apoptotic effects of high-dose vitamin C in cholangiocarcinoma cell line HTML (abstract.php?id=2160&aTitle=Antiproliferative and apoptotic effects of high-dose vitamin C in cholangiocarcinoma cell line) | Fulltext (../admin/12389900798187/2018_17_6_9.pdf)

Nuntiya Somparn (mailto:nuntiya_tom@hotmail.com), *Veerapol Kukongviriyapan*, *Suphaket Saenthaweesuk*,
http://dx.doi.org/10.4314/tjpr.v17i6.9
(http://dx.doi.org/10.4314/tjpr.v17i6.9)

Vitamin B2 blocks development of Alzheimerâ€™s disease in APP/PS1 transgenic mice via anti-oxidative mechanism HTML (abstract.php?id=2161&aTitle=Vitamin B2 blocks development of Alzheimerâ€™s disease in APP/PS1 transgenic mice via anti-oxidative mechanism) | Fulltext (../admin/12389900798187/2018_17_6_10.pdf)

Rong Zhao, *Huajun Wang*, *Chen Qiao*, *Kai Zhao* (mailto:xt1356@163.com),
http://dx.doi.org/10.4314/tjpr.v17i6.10
(http://dx.doi.org/10.4314/tjpr.v17i6.10)

Eupatilin attenuates diabetic nephropathy by upregulating matrix metalloproteinase-9 expression in diabetic rat kidney HTML (abstract.php?id=2162&aTitle=Eupatilin attenuates diabetic nephropathy by upregulating matrix metalloproteinase-9 ex<x>pression in diabetic rat kidney) | Fulltext (../admin/12389900798187/2018_17_6_11.pdf)

Linxin Xu, *Guoliang Shi*, *Yali Xu*, *Gang Lin*, *Wuzhou Zhang*, *Jing Yang* (mailto:jingyang6@hotmail.com),
http://dx.doi.org/10.4314/tjpr.v17i6.11
(http://dx.doi.org/10.4314/tjpr.v17i6.11)

Assessment of activity and mechanism of action of β-D-glucan against dengue virus HTML (abstract.php?id=2163&aTitle=Assessment of activity and mechanism of action of β-D-glucan against dengue virus) | Fulltext (../admin/12389900798187/2018_17_6_12.pdf)

Yonghong Song, *Wenzhi Zhang*, *Ravindran Jaganathan* (mailto:jravimicro@gmail.com),
http://dx.doi.org/10.4314/tjpr.v17i6.12
(http://dx.doi.org/10.4314/tjpr.v17i6.12)

Myricetin exerts potent anticancer effects on human skin tumor cells HTML (abstract.php?id=2164&aTitle=Myricetin exerts potent anticancer effects on human skin tumor cells) | Fulltext (../admin/12389900798187/2018_17_6_13.pdf)

Wei Sun, *Youming Tao* (mailto:tmilhollanaveka@yahoo.com), *Daojiang Yu*, *Tianlan Zhao*, *Lijun Wu*, *Wenyuan Yu*, *Wenya Han*,
http://dx.doi.org/10.4314/tjpr.v17i6.13
(http://dx.doi.org/10.4314/tjpr.v17i6.13)

Analysis of Coscinium fenestratum Colebr stem extract and effect of the extract on mean arterial blood pressure, heart rate and force of contraction in rats HTML (abstract.php?id=2165&aTitle=Analysis of Coscinium fenestratum Colebr stem extract and effect of the extract on mean arterial blood pressure, heart rate and force of contraction in rats) | Fulltext

Original Research Article | OPEN ACCESS

Co-crystalization of quercetin and malonic acid using solvent-drop grinding method

Dwi Setyawan (mailto:dwisetyawan-90@ff.unair.ac.id), *Rachel Olivia Jovita*, *Muhammad Iqbal*, *Abhimata Paramanandana*, *Helmy Yusuf*, *Maria LAD Lestari*

Department of Pharmaceutics, Faculty of Pharmacy, Universitas Airlangga, Surabaya 60286, Indonesia;

For correspondence:- Dwi Setyawan *Email:* dwisetyawan-90@ff.unair.ac.id (mailto:dwisetyawan-90@ff.unair.ac.id) *Tel:*+62315033710

Accepted: 19 May 2018 **Published:** 30 June 2018

Citation: *Setyawan D, Jovita RO, Iqbal M, Paramanandana A, Yusuf H, Lestari ML. Co-crystalization of quercetin and malonic acid using solvent-drop grinding method. Trop J Pharm Res 2018;* ***17(6)****:997-1002 doi: http://dx.doi.org/10.4314/tjpr.v17i6.3 (http://dx.doi.org/10.4314/tjpr.v17i6.3)*

Abstract

Purpose: To determine the physicochemical properties and in vitro dissolution profile of quercetin-malonic acid co-crystals prepared using solvent-drop grinding method.

Methods: Co-crystallization of quercetin (Q) and malonic acid (MA) in molar ratios of 1:1 (CC1) and 1:2 (CC2) was performed by solvent-drop grinding method with addition of 20 % (w/v) ethanol in a shaker mill run for 30 min. The co-crystal phase was characterized by differential scanning calorimetry (DSC), powder x-ray diffractometry (PXRD), scanning electron microscopy (SEM), and fourier transform infrared (FT-IR) spectroscopy. In vitro dissolution was performed using the paddle method at 100 rpm in the medium of citrate buffer (pH 5.0 ± 0.05) containing 2.0 % (w/v) sodium

medium of citrate buffer (pH 5.0 ± 0.05) containing 2.0 % (w/v) sodium lauryl sulfate at 37 ± 0.5 °C.

Results: Thermograms from DSC showed that CC1 and CC2 co-crystals had endothermic peaks at 283.02 and 266.61 °C, respectively. These peaks were in-between the melting points of Ma and Q. The powder diffractogram of CC1 showed new diffraction peaks at 16.21, 19.87, and 28.88 °, while CC2 showed new ones at 16.18, 19.86, and 28.83 °. There were OH- band shifts in IR spectra from 3411 to 3427 cm^{-1} for CC1, and from 3411 to 3466 cm^{-1} for CC2. Images from SEM indicate that the crystal habits and morphologies of the co-crystals differed from those of the original components. The dissolution efficiency of CC2 increased 1.056 times relative to pure Q.

Conclusion: Co-crystal phase of Q and MA prepared using solvent-drop grinding (CC1 and CC2) displays physicochemical characteristics different from those of the physical mixtures and their pure components. There is an increase in vitro dissolution as a result of co-crystal formation.

Keywords: Co-crystal, Dissolution, Malonic acid, Quercetin, Solvent-drop grinding

Impact Factor

Thompson Reuters (ISI): 0.569 (2016)
H-5 index (Google Scholar): 20

Article Tools

Share this article with

email address Share

- Article status: **Free**
- Fulltext in PDF (../admin/12389900798187/2018_17_6_3.pdf)
- Similar articles in Google (https://www.google.com.ng/?gfe_rd=cr&ei=JxO2VfnJOofe8gfy_4DYDQ&gws_rd=ssl#q=Co-crystalizati quercetin and malonic acid using solvent-drop grinding method)
- Similar article in this Journal:

Archives

Tropical Journal of Pharmaceutical Research June 2018; 17 (6): 997-1002
ISSN: 1596-5996 (print); 1596-9827 (electronic)
© Pharmacotherapy Group, Faculty of Pharmacy, University of Benin, Benin City, 300001 Nigeria.

Available online at http://www.tjpr.org
http://dx.doi.org/10.4314/tjpr.v17i6.3

Original Research Article

Co-crystalization of quercetin and malonic acid using solvent-drop grinding method

Dwi Setyawan*, Rachel Olivia Jovita, Muhammad Iqbal, Abhimata Paramanandana, Helmy Yusuf, Maria LAD Lestari

Department of Pharmaceutics, Faculty of Pharmacy, Universitas Airlangga, Surabaya 60286, Indonesia

For correspondence: **Email: dwisetyawan-90@ff.unair.ac.id; **Tel:** +6231-5033710; **Fax:** +6231-5020514*

Sent for review: 28 February 2018 *Revised accepted: 19 May 2018*

Abstract

Purpose: *To determine the physicochemical properties and in vitro dissolution profile of quercetin-malonic acid co-crystals prepared using solvent-drop grinding method.*
Methods: *Co-crystallization of quercetin (Q) and malonic acid (MA) in molar ratios of 1:1 (CC1) and 1:2 (CC2) was performed by solvent-drop grinding method with addition of 20 % (w/v) ethanol in a shaker mill run for 30 min. The co-crystal phase was characterized by differential scanning calorimetry (DSC), powder x-ray diffractometry (PXRD), scanning electron microscopy (SEM), and fourier transform infrared (FT-IR) spectroscopy. In vitro dissolution was performed using the paddle method at 100 rpm in the medium of citrate buffer (pH 5.0 ± 0.05) containing 2.0 % (w/v) sodium lauryl sulfate at 37 ± 0.5 °C.*
Results: *Thermograms from DSC showed that CC1 and CC2 co-crystals had endothermic peaks at 283.02 and 266.61 °C, respectively. These peaks were in-between the melting points of Ma and Q. The powder diffractogram of CC1 showed new diffraction peaks at 16.21, 19.87, and 28.88 °, while CC2 showed new ones at 16.18, 19.86, and 28.83 °. There were OH- band shifts in IR spectra from 3411 to 3427 cm^{-1} for CC1, and from 3411 to 3466 cm^{-1} for CC2. Images from SEM indicate that the crystal habits and morphologies of the co-crystals differed from those of the original components. The dissolution efficiency of CC2 increased 1.056 times relative to pure Q.*
Conclusion: *Co-crystal phase of Q and MA prepared using solvent-drop grinding (CC1 and CC2) displays physicochemical characteristics different from those of the physical mixtures and their pure components. There is an increase in vitro dissolution as a result of co-crystal formation.*

Keywords: *Co-crystal, Dissolution, Malonic acid, Quercetin, Solvent-drop grinding*

Tropical Journal of Pharmaceutical Research is indexed by Science Citation Index (SciSearch), Scopus, International Pharmaceutical Abstract, Chemical Abstracts, Embase, Index Copernicus, EBSCO, African Index Medicus, JournalSeek, Journal Citation Reports/Science Edition, Directory of Open Access Journals (DOAJ), African Journal Online, Bioline International, Open-J-Gate and Pharmacy Abstracts

INTRODUCTION

A co-crystal is a crystalline material formed by two or more molecules held together by weak interaction in the same lattice [1]. In the pharmaceutical field, it is formed between an active pharmaceutical ingredient (API) and a co-former without any intrinsic destruction, detachment or covalent bonding. Co-crystal components interact mostly through hydrogen bonding, but other weak bonding such as van der Waals and π-π interaction may not be ruled out [2]. A suitable co-former for co-crystal formation should possess functional groups that can form

hydrogen bonds; such groups include carboxylic acids, alcohols, amides, amines, and hydroxyl groups [3,4]. Co-crystallization involves numerous techniques in gas, liquid or solid phases. It is important to note that co-crystal phase grows either from the solution in solvent evaporation method or from molecular attachment in grinding method [5].

Grinding method in co-crystallization is divided into two techniques: dry and solvent-drop grinding. Dry grinding (mechanochemistry) is aimed at modifying crystalline phase formation through two mechanisms: molecular diffusion due to displacement, and cleavage planes formation in each cell unit. Solvent-drop grinding is performed by adding a small amount of specific solvent to the grinding process, an amount that can affect the process of co-crystal formation. Solvent-drop grinding possesses several advantages over dry grinding, including shorter time of co-crystal phase formation and possibility of obtaining pure co-crystal [6].

Quercetin (Q) is a flavonol which is ubiquitous in fruits and vegetables [7]. It has yellow, needle-shaped crystals with a molecular weight of 302.24 g/mol. Quercetin (Q) has two pKa values of 5.87 and 8.48, and a melting point of 326 °C [8-10]. The aqueous solubilities of anhydrous Q and its dihydrate form are 2.15 and 2.63 mg/L, respectively at 25 °C [11,12]. There are five hydroxyl groups in Q which confer strong antioxidant activity on the molecule, in contrast to other polyphenolic compounds [7]. However, Q belongs to class II in Biopharmaceutical Classification System (BCS) due to its low solubility in water and its good permeability [4]. The hydroxyl group in malonic acid (MA) molecular structure enables it to participate in hydrogen bonding two pKa values of MA are 2.83 and 5.70 which is appropriate to form co-crystal with quercetin [13].

This research was conducted in order to improve physicochemical properties and dissolution profile of Q by co-crystal formation. Co-crystallization was performed using solvent-drop grinding, with malonic acid (MA) as co-former.

EXPERIMENTAL

Materials

The major reagents used in this study were quercetin monohydrate (Tokyo Chemical Industry Co., Ltd., Japan, Lot: 83N20); malonic acid (E Merck, Germany); sodium lauryl sulfate (E Merck, Germany), and analytical grade of ethanol (E Merck, Germany).

Observation of co-crystal formation with hot stage microscopy (HSM)

Co-crystal formation was observed under an Optika B-383PL polarization microscope (Optika, Italy) equipped with an electric heater. A small quantity of Q was placed on an object glass with a cover glass. It was melted by heating and then left to recrystallize. Next, MA was placed on the edge of the glass cover. The sample was then re-heated until it melted completely. As it was melting, MA was slipped under the cover glass to make contact with the Q crystalline surface. The contact zone between Q and MA was observed for the growth of new crystalline phase under a polarization microscope at 100x magnification, and the images were captured using a digital camera.

Production of co-crystals by solvent-drop grinding method

The components Q and MA were weighed according to the desired molar ratios of 1:1 and 1:2 (CC1 and CC2, respectively), and then inserted into the grinding jar, along with 20 % (w/v) ethanol and grinding balls. The grinding jar was placed on the shaker mill and it was run for 30 min.

Preparation of physical mixture

The components Q and Ma were weighed in the molar ratio of 1:1 and 1:2 (PM1 and PM2 respectively), and then mixed homogeneously in a mortar.

Differential scanning calorimetry (DSC)

Analysis with DSC was performed to determine any differences in the melting points of Q, MA, PM1, and PM2. Each sample (ranging from 5 to 7 mg) was placed in an aluminium pan and hermetically sealed. The analysis was conducted using DSC 1000 (Linseis, Germany) over the temperature range of 50 - 350 °C at a heating rate of 10 °C/min.

Powder x-ray diffractometry (PXRD)

Powder x-ray diffraction was performed on Q, MA, PM1, PM2, CC1, and CC2 on Phillips X'pert diffractometer (Netherland) with CuKα radiation. Each sample was filled into a glass holder and levelled using a glass plate before placing in the x-ray device. The PXRD was performed in 2θ range of 5 - 40 ° at room temperature, at a voltage of 40 kV and current of 40 mA.

Fourier transform infrared (FT-IR) spectrophotometry

FT-IR spectroscopy was performed with Jasco 5300 FT-IR spectrophotometer (Jasco, USA) on Q, MA, PM1, PM2, CC1, and CC2. Sample powder was ground homogeneously with potassium bromide (KBr, spectroscopic grade) in a ratio of 1 % (w/w) and then pressed to form a disc which was placed in the sample holder and scanned at wavenumber range 4000 - 400 cm^{-1}.

Scanning electron microscopy (SEM)

Photographic images of Q, MA, CC1, and CC2 were captured using TM 3000 Tabletop Microscope (Hitachi, Japan). Each sample was placed on sample holder and coated with gold aluminium of thickness 10 nm. Morphological observation was carried out at appropriate magnification at a voltage of 20 kV and current of 12 mA.

In vitro dissolution studies

In vitro dissolution studies were carried out on Q, PM1, PM2, CC1, and CC2 using Erweka DT 700 (Erweka, Germany) equipped with paddle apparatus. The dissolution medium was citrate buffer (pH 5.0 ± 0.05) with 2.0 % (w/v) sodium lauryl sulfate (SLS) to achieve sink condition. A sample of Q (20 mg) was added to 900 mL dissolution medium and stirred at paddle speed of 100 rpm and temperature of 37 ± 0.5 °C. Then, 5.0 mL of the sample was collected at 5, 10, 15, 30, 45 and 60 min and filtered through 0.45 µm diameter millipore. The absorbance of the filtrate was read at 286 nm in a UV-Vis spectrophotometer. The concentration Q was calculated from a standard calibration curve. Each sample was analysed in triplicate.

RESULTS

HSM identification

The result of co-crystal identification by HSM method are presented in Figure 1. It can be seen that Q showed small columnar shape, while MA showed plate shape characteristics. The contact zone between the two components showed a new crystalline phase in fibrous shape that indicated new crystal (co-crystal) formation.

DSC thermograms

The thermal behaviours of Q, MA, CC1, and CC2 as characterized by DSC are shown in Figure 2. It reveals that Q and MA had melting points at 321.92 and 135.07 °C, respectively, and CC1 thermogram showed endothermic peaks at 95.69, 184.35, 283.02, and 312.70 °C, while CC2 thermogram showed endothermic peaks at 100.02, 125.64, 132.29, 183.97, 266.61, and 302.26 °C. The new endothermic peak at 283.02 and 266.61 °C for CC1 and CC2, respectively indicated the formation of co-crystals.

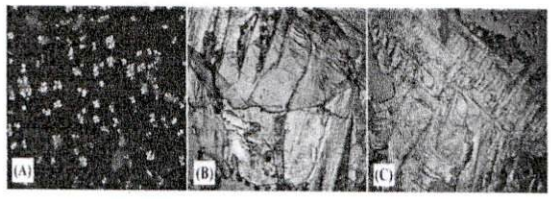

Figure 1: Crystal images obtained from polarization microscope with x100 magnification of Q (A), MA (B), and Q-MA (C) contact zones

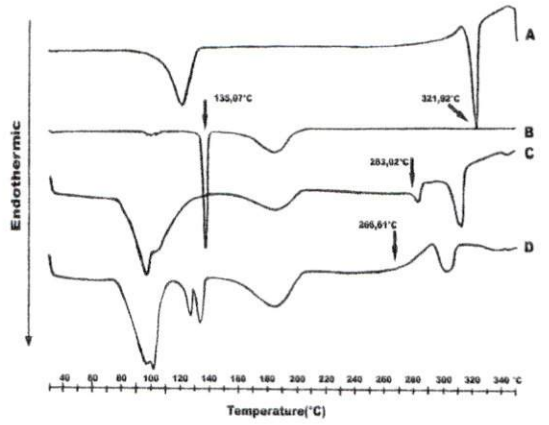

Figure 2: Thermograms of Q (A), MA (B), CC1 (C) and CC2 (D)

Powder diffractograms

The powder diffraction profiles of Q, MA, PM1, PM2, CC1 and CC2 are shown in Figure 3. Pure samples of Q and MA showed a number of sharp diffraction peaks at a certain 2θ degree. However, diffractograms of PM1 and PM2 revealed superimposed pattern from both of components. On the other hand, CC1 and CC2 generated new diffraction peaks at 2θ (16.21, 19.87, and 28.88 ° for CC1; and 16.18, 19.86, 28.83 ° for CC2). The new diffraction peaks on both CC1 and CC2 corresponded to formation of new crystalline phases.

FT-IR spectra

The IR spectra of Q, MA, PM1, PM2, CC1, and CC2 are presented in Figure 4. The IR spectra of CC1 and CC2 showed different profiles from those of the pure components, and also from those of the physical mixtures. The OH- group

band of Q shifted to higher wave number in co-crystal phase spectra, from 3411 to 3427 cm^{-1} in CC1, and to 3466 cm^{-1} in CC2. Furthermore, the peak of C=O group in Q at 1667 cm^{-1} and 1612 cm^{-1} disappeared and shifted to 1638 cm^{-1} in CC2 spectra.

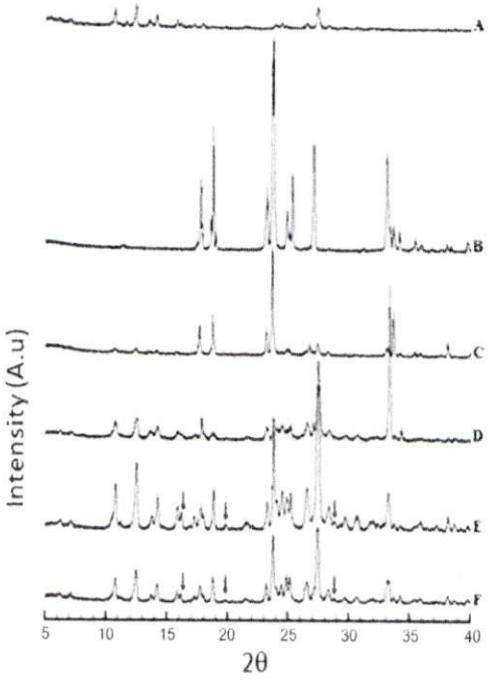

Figure 3: Comparison of x-ray diffractogram of Q (A), MA (B), PM1 (C), PM2 (D), CC1 (E), and CC2 (F)

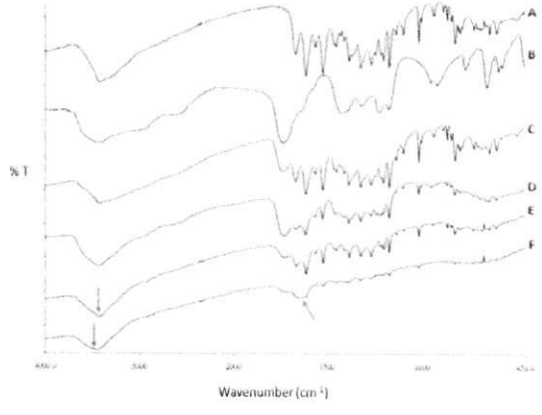

Figure 4: FT-IR spectra of Q (A), MA (B), PM1 (C), PM2 (D), CC1 (E), and CC2 (F). ↓ indicates band shift in wavenumber

SEM photographs

Changes in Q-MA co-crystal surface morphology are shown in SEM photographs (Figure 5). At x1500 magnification, Q showed needle-shaped crystal, while MA yielded pebble-shaped crystals at x300 magnification. The morphologies of CC1 and CC2 were different from those of the pure components. It was also found that Q lost its habit crystal in CC1 and CC2, indicating the formation of new crystalline phase (co-crystal).

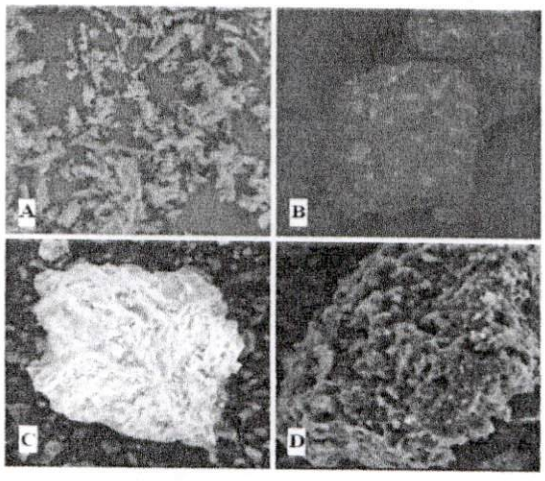

Figure 5: Microphotography of Q (A), MA (B), CC1 (C), and CC2 (D)

In vitro dissolution

The dissolution profiles of Q, PM1, PM2, CC1, and CC2 are shown in Figure 6. Both co-crystal phases (CC1 and CC2) showed slight improvement in dissolution profile when compared with their physical mixtures (PM1 and PM2), and pure Q.

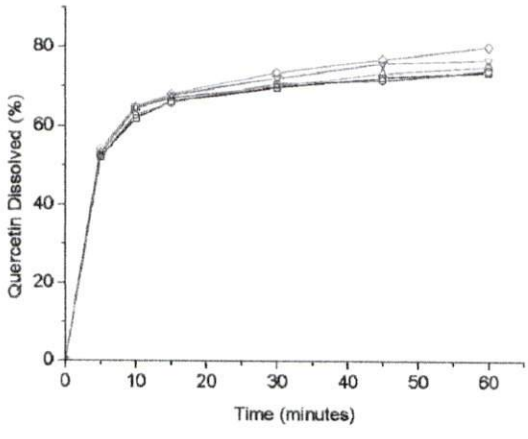

Figure 6: Dissolution rate profiles of Q (-□-), PM1 (-○-), PM2 (-Δ-), CC1 (-▽-), and CC2 (-◊-)

DISCUSSION

The HSM method was used as preliminary screening to detect new crystalline phase formation between Q and MA. Recrystallized Q and MA yielded different shape and colours

when observed under polarization microscope. Variation in colour are influenced by the intensity of light, fragment orientation and the thickness of the beam transmitted by the crystalline phase [14]. The new crystalline phase found in the contact zone is suspected to be a co-crystal phase formed between Q and MA [14].

The phase diagram of Q and MA generated a curve consistent with an incongruent system (unpublished data). In addition, the physical mixture of Q and MA at various composition ratios showed new endothermic peaks in the range of 277.87-282.15 °C, along with endothermic peaks of Q and MA. Endothermic peaks for 20:80 and 90:10 weight ratios of Q and MA were found in the temperature range of 277.87-282.15 °C. A binary system that forms an incongruent diagram indicates a possible interaction between components in the system [15]. Based on this fact, co-crystal formation of Q-MA with 1:1 and 1:2 molar ratios (CC1 and CC2 respectively) was carried out. A dehydration event was seen for Q at ~120 °C, and the same event was observed in CC1 and CC2 by endothermic peak at 95.69 and 100.02 °C, respectively. A new endothermic peak appeared in-between the melting point of Q and MA. This indicates the formation of co-crystal phase. It is known that a decrease in melting point illustrates interaction between two components in solid state [14].

Co-crystal formation between Q and MA was also established through PXRD analysis. The sharp diffractions observed for Q and MA suggests that both components were in crystalline form [10]. The superimposed patterns of Q and MA in PM1 and PM2 diffractograms indicate absence of interaction between both components, while the new peaks observed in CC1 and CC2 diffractograms suggest that Q and MA interacted under solvent-drop grinding to form co-crystal phase [14].

Hydrogen bonding is the main indicator in co-crystal formation which can be detected through IR spectrum from peak shifts, reduction in peak intensity, and disappearance or appearance of certain peaks [16]. Shifts in OH- and C=O groups of Q in CC1 and CC2 suggest co-crystal formation. Using ChemDraw® Ultra 12.0.2.1076, it was found that hydrogen bonding between Q and MA was more likely to occur between O-H in aromatic ring A or aromatic ring B of Q with O-H of carboxylic group of MA. This hypothesis was based on the low amount of total energy produced by MA-Q ring A and MA-Q ring B (99.22 kcal/mol and 43.85 kcal/mol, respectively).

Dissolution efficiency describes the amount of drug dissolved up to a certain time interval, and the entire dissolution process. It was used to calculate improvement in Q dissolution in 60 minutes (DE_{60}) and the result showed a slight improvement in CC2 dissolution (1.056 times) relative to Q.

The co-crystal phase-induced improvement in solubility is hypothetically caused by new hydrogen bonding between Q and MA molecules [16]. The presence of co-former molecule within the crystal lattice leads to a change in conformational packing or crystal habit which may affect chemical properties of a material, such as solubility and dissolution rate [17]. In addition, the presence of MA hydrogen-bonded to Q will facilitate contact between drug molecules and water, thereby increasing drug solubility [14].

CONCLUSION

Co-crystal of Q-MA can be formed in 1:1 and 1:2 molar ratio by the solvent-drop grinding method. The co-crystal phases demonstrate increased *in vitro* dissolution rate compared to Q and the physical mixtures. Due to variations in the physicochemical characteristics of quercetin-malonic acid cocrystal, it can be readily compressed into suitable solid dosage forms.

DECLARATIONS

Conflict of Interest

No conflict of interest associated with this work.

Contribution of Authors

The authors declare that this work was done by the authors named in this article and all liabilities pertaining to claims relating to the content of this article will be borne by them.

REFERENCES

1. *Sanjay A, Manohar D, and Bhanudas S. Pharmaceutical cocrystallization: a review. J Adv Pharm Educ Res. 2014; 4(4): 388–396.*
2. *Karagianni A, Malamatari M, and Kachrimanis K. Pharmaceutical Cocrystals: New Solid Phase Modification Approaches for the Formulation of APIs. Pharmaceutics. 2018; 10(18): 1-30.*
3. *Kothur RR. Swetha AS, and Bondili NP. An Outline of Cocrystal Engineering of Pharmaceutical Co-crystals and Applications: A Review. IJPRD. 2012; 4(08): 084-092.*

4. Pujari TA. Cocrystals of nutraceuticals: protocatechuic acid and quercetin. USF: Thesis. 2009; 101.
5. Nanjwade VK, Manvi FV, Shamrez Ali M, Basavaraj K, and Maste M. New Trends in the Co-crystallization of Active Pharmaceutical Ingredients. J Appl Pharm Sci. 2011; 01(08): 01-05.
6. Trask AV and W. Jones W. Crystal engineering of organic cocrystals by the solid-state grinding approach. Top Curr Chem. 2005; 254: 41–70.
7. Materska M. Quercetin and its Derivatives: Chemical Structure and Bioactivity - a Review. Polish J Food Nutr Sci. 2008; 58(4): 407–413.
8. Brewer KJ. The Merck Index: An Encyclopedia of Chemicals, Drugs, and Biologicals, 14th ed. Edited by Maryadele J. O'Neil (Editor), Patricia E. Heckelman (Senior Associate Editor), Cherie B. Koch (Associate Editor), and Kristin J. Roman (Assistant Editor). J Am Chem Soc. 2007; 129(7): 2197–2197.
9. Daniel S, Allen G, and Raj G. Static quenching of ruthenium(II)-polypyridyl complexes by gallic acid and quercetin in aqueous and micellar media. Int Lett Chem Phys Astron. 2014; 13(1): 21–31.
10. Kakran M, Sahoo NG, Li L, and Judeh Z. Fabrication of quercetin nanoparticles by anti-solvent precipitation method for enhanced dissolution. Powder Technol. 2012; 223: 59-64.
11. Srinivas K, King JW, Howard LR, and Monrad JK. Solubility and solution thermodynamic properties of quercetin and quercetin dihydrate in subcritical water. J Food Eng. 2010; 100(2): 208-218.
12. Vasisht K, Chadha K, Karan M, Bhalla Y, Jena AK, and Chadha R. Enhancing biopharmaceutical parameters of bioflavonoid quercetin by cocrystallization. Cryst Eng Comm. 2016; 18(8): 1403–1415.
13. Strittmatter H, Hildbrand S, and Pollak P. Malonic Acid and Derivatives. Ullmann's Encyclopedia of Industrial Chemistry. Berlin: Wiley-VCH Verlag GmbH & Co. KGaA., 2007, [cited 2017 Dec 8]. Available from : https://doi.org/10.1002/14356007.a16_063.pub2.
14. Setyawan D, Sari R, Yusuf H, and Primaharinastiti R. Preparation and characterization of artesunate - Nicotinamide cocrystal by solvent evaporation and slurry method. Asian J Pharm Clin Res. 2014; 7(1): 62–65.
15. Yamashita H, Hirakura Y, Yuda M, Teramura T, and Terada K. Detection of Cocrystal Formation Based on Binary Phase Diagrams Using Thermal Analysis. Pharm Res. 2013; 30(1): 70–80.
16. Veverka M, Dubaj T, Gallovič J, Jorík V, Veverková E, Danihelová M, and Šimon P.. Cocrystals of quercetin: synthesis, characterization, and screening of biological activity. Monatsh Chem. 2015; 146(1): 99-109.
17. Bauer J, Spanton S, Henry R, Quick J, Dziki W, Porter W, and Morris J. Ritonavir: An Extraordinary Case of Conformational Polymorphism. Pharm Res. 2001; 18(6): 859–866.

Editorial Board

Archives